

Phase transition in an out-of-equilibrium monolayer of dipolar vibrated grainsLoreto Oyarte,¹ Pablo Gutiérrez,² Sébastien Aumaître,^{2,*} and Nicolás Mujica¹¹*Departamento de Física, Facultad de Ciencias Físicas y Matemáticas, Universidad del Chile, Avenida Blanco Encalada 2008, Santiago, Chile*²*Service de Physique de l'Etat Condensé, DSM, CEA-Saclay, CNRS, 91191 Gif-sur-Yvette, France*

(Received 17 July 2012; published 13 February 2013)

We report an experimental study on the transition between a disordered liquidlike state and an ordered solidlike one, in a collection of magnetically interacting macroscopic grains. A monolayer of magnetized particles is vibrated vertically at a moderate density. At high excitation a disordered, liquidlike state is observed. When the driving dimensionless acceleration Γ is quasistatically reduced, clusters of ordered grains grow below a critical value, Γ_c . These clusters have a well-defined hexagonal and compact structure. If the driving is subsequently increased, these clusters remain stable up to a higher critical value, Γ_l . Thus, the solid-liquid transition exhibits a hysteresis cycle. However, the lower onset Γ_c is not well defined as it depends strongly on the acceleration ramp speed and also on the magnetic interaction strength. Metastability is observed when the driving is rapidly quenched from high acceleration, $\Gamma > \Gamma_l$, to a low final excitation, Γ_q . After this quench, solid clusters nucleate after a time lag, τ_o , either immediately ($\tau_o = 0$) or after some time lag ($\tau_o > 0$) that can vary from seconds up to several hundreds of seconds. The immediate growth occurs below a particular acceleration value, Γ_s ($\lesssim \Gamma_c$). In all cases, for $t \geq \tau_o$ a solid cluster's temporal growth can be phenomenologically described by a stretched exponential law. The evolution of the parameters of this law as a function of Γ_q is presented and the values of fitted parameters are discussed.

DOI: [10.1103/PhysRevE.87.022204](https://doi.org/10.1103/PhysRevE.87.022204)

PACS number(s): 45.70.-n, 05.70.Ln

I. INTRODUCTION

Granular matter dissipates energy by friction and inelastic collisions, therefore an external driving is necessary to observe dynamical behaviors. Despite their intrinsic macroscopic and nonequilibrium nature, the resulting excited state, from granular gas to an ordered compact set of grains, often shares similarities with thermal systems described by statistical physics at equilibrium. However, important nonequilibrium features emerge, like the absence of a universal effective temperature, deviations from Fourier's conduction law, spatiotemporal instabilities, the absence of scale separation, and so forth. Granular matter is therefore a good candidate in which to study nonequilibrium phase transitions between these different excited states [1,2].

The transition of granular media from liquidlike to solidlike states has already been reported. Under shearing or vertical tapping, monodisperse spheres tend to collectively organize themselves in the most dense crystal state [3–6]. When a monolayer of grains that is confined between two horizontal plates is vibrated vertically, unexpected ordered structures nucleate from the liquid state at high excitation [7–9]. This phase separation is driven by the negative compressibility of the effective two-dimensional fluid, as in the van der Waals model for molecular fluids [9].

In the present experiment, we are concerned with granular systems where another interaction is added to the usual hard sphere collisions. To do so, we use premagnetized spheres. Magnetized spheres have been studied under an external applied magnetic field [10,11]. When a set of these magnetized spheres, compacted by gravity, is submitted to a vertical magnetic field, the surface of the granular packing is

destabilized above a given onset and forms peaks [10]. When a granular gas is submitted to an increasing horizontal magnetic field at a given excitation, a transition to a clustered state is observed [11]. A mixture of magnetic and nonmagnetic spheres has been also studied in a configuration similar to ours, but at a lower surface fraction of the magnetic particles and in a horizontal plate with no top lid, which limits the energy injection as the system is kept in a quasi-two-dimensional state. In this mixed system, authors have focused on the existence and the growth in time of clusters composed of solely magnetic particles, in the bath of nonmagnetic ones, as a function of control parameters [12,13].

In our study, no external field is added and the remanent magnetic moment, present in all the particles, generates a dipolar interaction between them. This kind of two-dimensional (2D) dipolar liquid [with three-dimensional (3D) magnetostatics] has been extensively studied numerically in order to understand the transition from isolated to branched chains [14–16]. Compared to our experiments, an important difference is that these numerical studies are performed at equilibrium. Also, they use a lower surface density, $\phi = N\pi d^2/(4L^2) \approx 0.3-0.4$ (where d is the particle diameter, N is the number of particles, and L is the system size). Numerical studies also introduce the reduced temperature $T^* = k_B T/(\mu^2/d^3)$, where μ is the particle's magnetic moment. Although it was not easy to estimate it in our experiments, we verified at least that the attractive force between particles with aligned moments is weak. Actually, two particles have to be almost in contact to get an attraction that overcomes their own weight, meaning that $\mu^2/d^3 \sim mgd$, with m being their mass and g the gravity acceleration. Therefore T^* can be crudely estimated by $T^* \sim m(A\omega)^2/(\mu^2/d^3)$, using a granular temperature proportional to the energy per grain, provided by a vibration of amplitude A and angular frequency ω , and using $\mu^2/d^3 \sim mgd$. One gets $T^* \sim \Gamma A/d \sim 0.2-0.6$, which

*Corresponding author: sebastien.aumaitre@cea.fr

is actually in the temperature range accessible numerically. A comparison between experiments and numerical studies seems promising.

Here, we present an experimental study of the behavior of a layer of premagnetized particles at low density, i.e., constituting a sub-monolayer occupying only slightly more than half of the cell surface. Particles are confined in a shallow geometry, with a height that is small compared to the horizontal dimensions. The system is therefore quasi-2D with 3D magnetostatics. The experimental cell is submitted to vertical vibration, the control parameter being the dimensionless acceleration $\Gamma = A\omega^2/g$, which is varied keeping constant the driving frequency ω .

This paper is organized in the following way: a description of our experimental device and procedures is presented in Sec. II. Then, we present first, in Sec. III A, the behavior of the system when the control parameter Γ is *quasistatically* reduced or increased. Below a critical value of Γ , clusters organize in a hexagonal lattice. A hysteretic behavior is observed whether the acceleration of the cell is increased or decreased. In Sec. III B, we present results starting from a liquidlike state, from which we quench the system into the hysteresis region in order to study the dynamical growth of the ordered phase. After presenting our experimental observations on the dynamical evolution of solid clusters, we show that their growth can be fitted by a stretched exponential law. The evolution of the parameters of this law as a function of the quenched acceleration is presented and the values of fitted parameters are discussed. In the last section, Sec. IV, we present a discussion of our results as well as our conclusions. Some future perspectives are also outlined.

II. EXPERIMENTAL SETUP AND PROCEDURES

The experimental device, illustrated in Fig. 1, is similar to the one presented in Refs. [17,18]. Stainless steel spheres (type 422) of diameter $d = 1$ mm are confined between two horizontal glass plates, which have an indium titanium oxide (ITO) coating layer to prevent static electricity (resistivity,

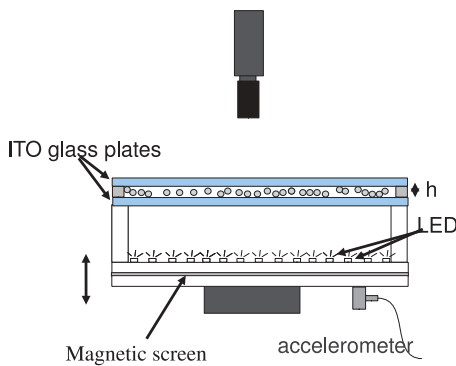


FIG. 1. (Color online) Sketch of the experimental setup. The cell contains the quasi-2D box where grains are confined between two ITO-coated glass plates. The box is placed above an array of light-emitting diodes and a camera takes pictures of the particles from above. An accelerometer measures the applied dimensionless acceleration $\Gamma = A\omega^2/g$.

$7.5 \times 10^{-6} \Omega\text{m}$; thickness, 25 nm). The dimensions of the cell are as follows: the gap between the plates, $h = 1.8d$; and lateral dimensions, $L_x = L_y = L = 100d$. The cell is submitted to sinusoidal vibration $z(t) = A \sin(\omega t)$, provided by an electromagnetic shaker. We take care to screen its magnetic field. The cell is illuminated from below by an array of light-emitting diodes. A camera takes pictures from the top. Typical images are shown in Fig. 2. Almost all particles are tracked using an open source MATLAB code [19], which works well for the sub-monolayer surface filling fractions that are used. The cell acceleration, $a(t) = \ddot{z}(t)$, is measured with a piezoelectric accelerometer fixed to the base. Our control parameter is the dimensionless acceleration $\Gamma = A\omega^2/g$. Results presented here have been obtained with the filling fraction density $\phi = 0.59$, where $N = 7372$ is the number of spheres, frequency $f = \omega/2\pi = 100$ Hz, period of base oscillation $P = 1/f = 0.01$ s, and $\Gamma = 3\text{--}5.3$. We have verified that the phenomenology is not qualitatively affected by the number of particles as long as the system is not too dense.

A major experimental challenge is to keep constant the magnetization of the spheres. Indeed, depending on the magnetization procedure, some shifts occur for the acceleration onset values, although the qualitative behavior of the system remains the same. Grains are magnetized by contact with a strong Neodyme magnet. Some additional thermal treatments have also been probed to maintain the magnetization. The magnetic moment acquired by the spheres is partially lost when the system is vibrated for long times. This loss of interaction strength is produced by collisions and local particle heating. This issue is discussed in more detail below, in particular, when we present experimental results of quasistatic acceleration ramps.

Starting from a homogeneous liquid state at $\Gamma = 5$, and decreasing A at ω fixed, we observe that for $\Gamma \leq 3.4$ clusters of ordered grains grow almost immediately, as shown in Fig. 2 (right panel). In contrast to numerical simulation predictions where all particles form chains [14–16], here clustered particles are well organized in a 2D triangular crystal, except at the edge of the cluster where more linear chains coexist with disordered liquidlike particles. In fact, the precise cluster's topology depends on Γ and the speed at which the solid cluster grows. For rapid changes in driving from high acceleration to $\Gamma \sim 1\text{--}3$, the solid phase will grow quickly and will be first formed by many subclusters separated by defects as well as many linear chains. However, if driving is varied slowly from a liquid state, a single cluster will first nucleate and then grow slowly, with a smaller amount of defects, like the one shown in Fig. 2 (right panel).

We used Delaunay triangulation, which relates three nearest neighbors, in order to define the number of particles belonging to a cluster, N_c . Several triangles coincide with a particle, and if at least one of them has an area, \mathcal{A} , smaller than $0.5d^2$, then the particle is assumed to be in a cluster. The precise value of the onset does not modify qualitatively the results presented here. It has been chosen in order to find all the particles inside a cluster in the cell, as in the example shown in Fig. 2 (right panel). Some particles in the liquid phase will inevitably fit this condition as well. This will add a background noise of

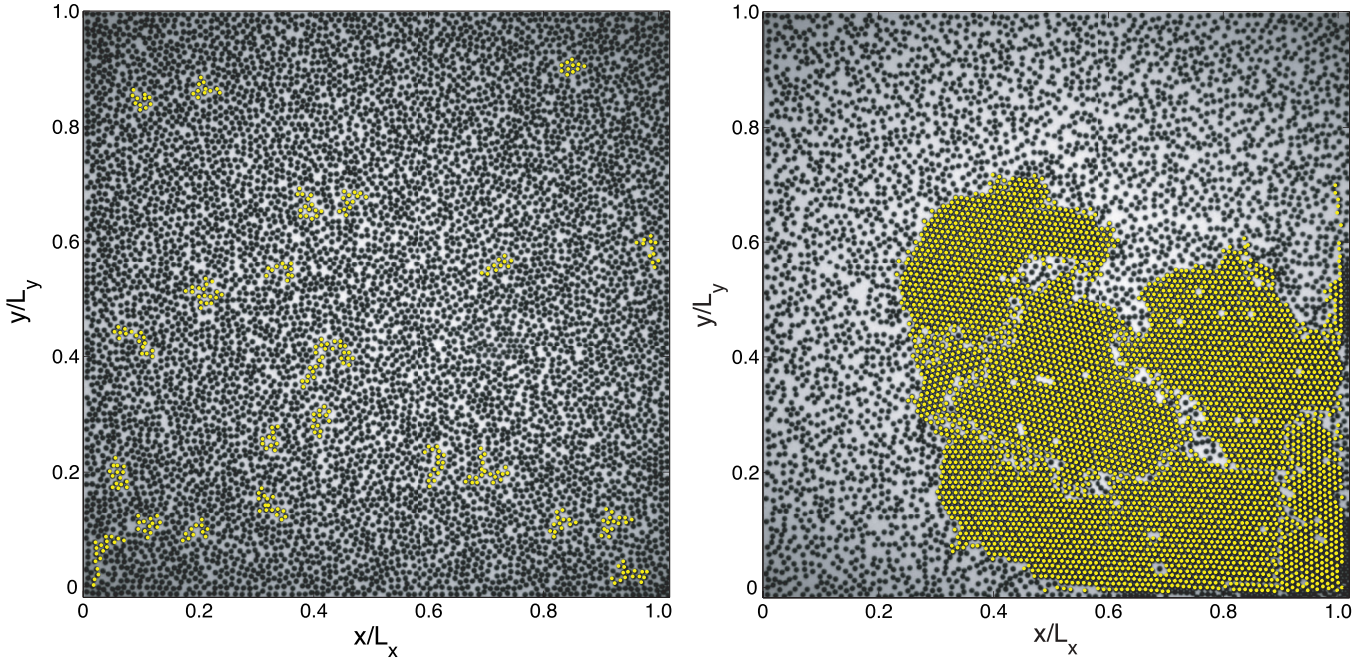


FIG. 2. (Color online) Left: Disordered liquid-state snapshot, $\Gamma = 5$. Yellow (white) dots show groups of more than 10 particles that meet the criterion used for defining particles in a solid cluster. In this liquid state, these clusters are continuously forming and disappearing, tracing density fluctuations. Right: Coexistence of solid and liquid phases, $\Gamma = 3.5$. The solid cluster presents a hexagonal order. It is about two-thirds of its final size. Eventually, it will be composed of about 6500 particles, approximately 85% of all particles.

about 1000 particles belonging to small unstable, short-living clusters. As shown in Fig. 2 (left panel), it is the trace of density fluctuations in the liquid phase.

III. EXPERIMENTAL RESULTS

A. Quasistatic acceleration ramps

We first present results obtained performing *quasistatic* cooling and heating ramps, by slowly decreasing and increasing the driving acceleration, respectively. In Fig. 3, we plot the fraction of particles inside a cluster, N_c/N , as a function of Γ . Black symbols represent the fraction of crystallized particles when the acceleration is slowly decreased from the liquid state, whereas green (gray) ones represent this quantity when the acceleration is slowly increased. Each similar pair of symbols corresponds to different experimental realizations. More precisely, the procedure is the following. First the system is set at high acceleration ($\Gamma \approx 5$). The system is left to evolve to a stationary state during a waiting time, t_w . Then, five images are acquired at a rate of 1 fps. Immediately after, Γ is reduced by a small amount and the system is again left to evolve during t_w until the next acquisition of images. This procedure is repeated until we reach the lowest acceleration of about $\Gamma = 3.1$. Then, the same procedure is used but Γ is increased until the completely fluidized state is obtained again. For most of the symbols in Fig. 3, $t_w = 15$ s (i.e., $t_w = 1500P$). For one case [black and green (black and gray) diamonds in Fig. 3], the acceleration was first increased up to the gas state and then decreased. No difference in the resulting curves is observable for a loop realized in this opposite way. In two cases, the waiting times are different: ramps with waiting times of 30 s

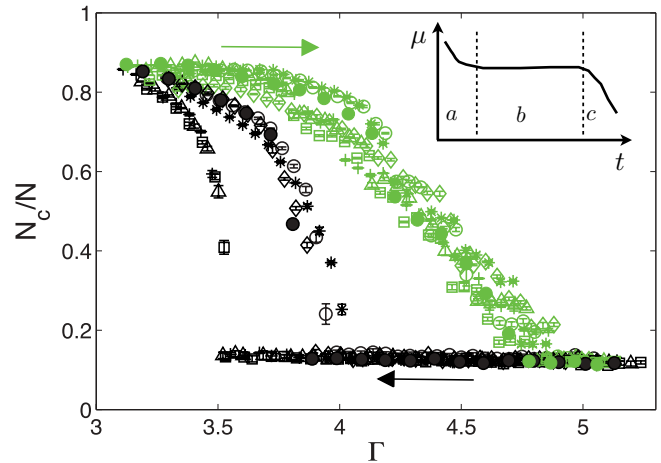


FIG. 3. (Color online) Fraction of particles inside a cluster N_c/N as function of Γ . Acceleration is varied quasistatically. Black and green (black and gray) symbols indicate the results when Γ is reduced and increased, respectively. Several ramps are shown for different realizations. Each pair of symbols corresponds to a closed Γ loop, performed in this order: $\circ, \circ, *, *, \diamond, \diamond, +, +, \Delta, \Delta, \square, \square, \bullet, \bullet$. For each ramp, Γ is varied with a waiting time of 15 s before obtaining images during 5 s at 1 fps. There are two exceptions: ramps for 30 s ($+, +$) and 180 s (\bullet, \bullet) waiting times. Magnetization is reduced after many hours of experiments, evident in some of the decreasing ramps ($+, \Delta, \square$), where the transition Γ is reduced, although not so in their correspondent increasing ramps ($+, \Delta, \square$). The last two ramps correspond to a longer waiting time (180 s, \bullet, \bullet) for which the transition point again is practically the same as before. Inset: schematic representation of magnetic moment dependence on time.

$[t_w = 3000P$: black and green (black and gray) crosses] and 180 s $[t_w = 18000P$: black and green (black and gray) solid circles]. In the caption of Fig. 3, we indicate the order in which these ramps were realized. Particles were not remagnetized during all the experiments presented in this figure.

The inset of Fig. 3 shows a schematic representation of the variation of the average magnetic dipole moment μ with time. Here, “time” means vibration oscillations, i.e., time during which the particles are in a fluidized collisional state at a given Γ . Three stages are identified (*a*, *b*, and *c*), and the vertical dotted lines indicate the transitions between them. The exact positions of the different transitions depend on Γ and the particular magnetization procedure. Stage *a* is characterized by a fast decrease of μ ; for $\Gamma \sim 5$, this can endure for a few tenths of a minute. Later, stage *b* corresponds to a stable average magnetization, which typically lasts for several hours. And finally, after many particle collisions, μ continues to decay.

The main result of Fig. 3 is that, for the current cooling and heating rates and procedure, there is a stable loop with two transition points: from a homogeneous liquid to a solid-liquid coexistence at $\Gamma_c = 3.9 \pm 0.1$, and from a solid-liquid coexistence to the homogeneous liquid state at $\Gamma_l = 4.8 \pm 0.1$. Thus, when the driving is slowly increased, the last cluster disappears always at a critical value which is higher than the value at which the first crystal appears when the driving is decreased: $\Gamma_l > \Gamma_c$. We refer to this loop as the *quasistatic hysteresis loop* (stage *b*), although it is not reproducible for very long experiments because of a reduction in the particle’s magnetization (stage *c*).

Indeed, some curves obtained for decreasing ramps have different Γ_c values as shown by the symbols $+$, Δ , and \square in Fig. 3. These shifted curves, which result in a lower transition acceleration value ($\Gamma_c \approx 3.5$) from the liquid state to the coexistence of solid and liquid phases, correspond to later runs without remagnetization in between. Therefore, these shifts are mainly due to particle demagnetization. However, for such runs, Γ_l does not change. We remark that when the waiting time t_w is increased to 180 s (18 000 P), black and green (black and gray) solid circles in Fig. 3, even with a lower magnetization, the previous hysteric cycle is recovered. It seems that for a lower magnetization and with $t_w = 1500P$ or $t_w = 3000P$, we do not wait enough to obtain the crystal growth. Thus, the loss of magnetization seems to increase the time necessary to get a quasistationary state. However, beyond this variability, the main qualitative feature remains the hysteric behavior with $\Gamma_c < \Gamma_l$.

Finally, measurements not shown here that are performed just after remagnetization (stage *a*) show that both Γ_c and Γ_l are shifted to higher values, whereas measurements made later, for very long experimental times after magnetization (very late times in stage *c*), present both Γ_c and Γ_l shifted to lower values.

B. Quench experiments

Knowing the onset of crystallization, we now study the dynamics when the homogeneous liquid phase is quenched. Starting from $\Gamma = 5$, we reduce suddenly the driving to a final value Γ_q between 3 and 4.5. We then acquire images at a low frame rate (0.5 fps) for several minutes. The typical measurement time is 10 min ($t_m = 6 \times 10^4 P$) in order to keep

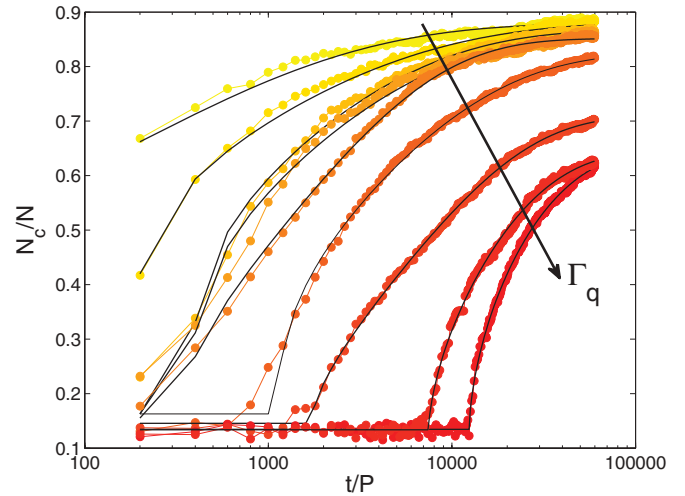


FIG. 4. (Color online) Fraction of particles that form part of a solid cluster, N_c/N , versus time t/P , for several Γ_q (quenched state). Initial time $t = 0$ corresponds to the moment Γ is abruptly quenched from $\Gamma = 5$ to Γ_q . For each run, images are acquired during 10 min, equivalent to $6 \times 10^4 P$. From left to right $\Gamma_q = 3.15, 3.31, 3.42, 3.53, 3.63, 3.74, 3.94, 4.13$, and 4.02 . For $\Gamma_q = 3.80$ and 4.2 there was no transition within the observation time. Continuous lines show fits for stretched exponential growth law, Eq. (1). On average, for increasing Γ_q , τ and τ_o increase and N_∞ decreases.

constant the particle’s magnetic dipole moment during the complete run (that is, for all the quenches), although some runs with $t_m = 20$ min have also been realized ($t_m = 1.2 \times 10^5 P$). For each image, we compute N_c , the total number of particles that belong to a solid cluster.

The temporal evolution of N_c is shown in Fig. 4 for different values of Γ_q . This series of quench experiments was performed in between the quasistatic loops identified by black diamonds and crosses in Fig. 3. Two time scales are clearly present: a growth time, τ , and a time lag, τ_o . Clusters grow slower for higher Γ_q . For $\Gamma_q \lesssim 3.4$, clusters grow immediately ($\tau_o = 0$); for higher Γ_q , cluster’s nucleation is delayed ($\tau_o > 0$). This allows us to define for this realization $\Gamma_s \approx 3.4$ as the acceleration below which $\tau_o \approx 0$. In the case $\tau_o > 0$ the system is metastable: it can be either in a homogeneous liquid phase or in a solid-liquid phase separated state. The transition from the former to the latter occurs if there is a density fluctuation strong enough to nucleate crystallization. Additionally, this density fluctuation has to have particles aligned in such a way that they can bind together. As Γ_q approaches Γ_l , this fluctuation has to be stronger (more dense), because the granular temperature is higher. Thus, it becomes less probable too. However, at the same time, its final size is smaller, requesting less binding energy. The corresponding lag time τ_o becomes usually larger, but its dependence on the appearance of the correct density fluctuation makes it highly variable from one realization to another. The general results are valid for every quench experiment done in the stable hysteresis loop: For Γ_q approaching Γ_l , the crystal growth time τ increases, the asymptotic number of particles in the solid phase decreases, and the lag time τ_o seems to increase on average but its variance seems to increase too (many more independent realizations are needed to study τ_o properly).

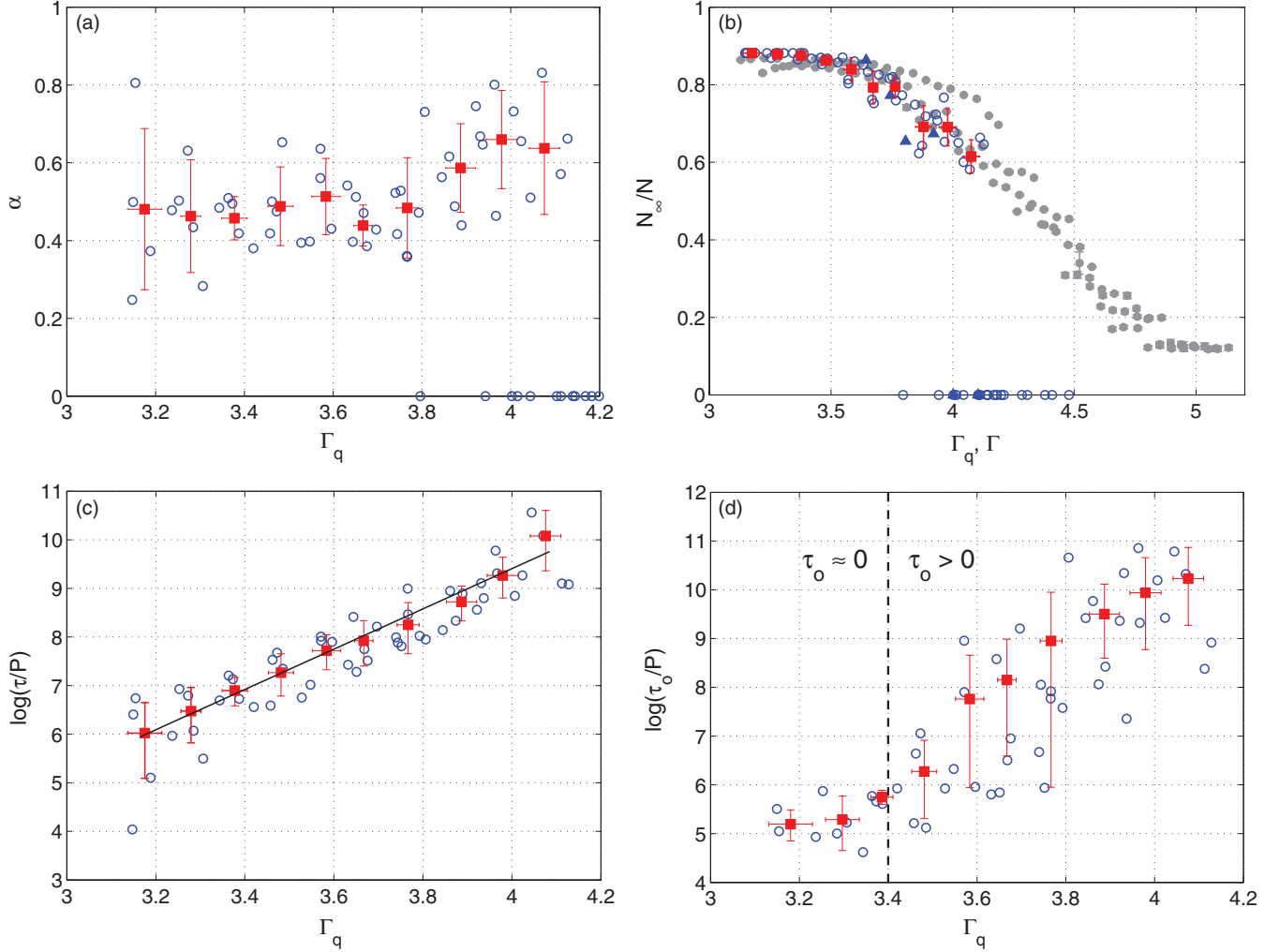


FIG. 5. (Color online) Fitted parameters α (a), N_∞ (b), τ (c), and τ_o (d) as functions of Γ_q . For panels (a) and (b) symbols on the x axis correspond to realizations for which the phase separation was not achieved in the experimental observation time. Open circles (\circ) represent raw data obtained from several independent ramps, whereas solid squares (\blacksquare) correspond to averages using 10 equal size windows in the complete Γ_q data range. Error bars were computed from standard deviations of the experimental points in each window. In panel (b), open circles (\circ) have a total measurement time $t_m = 6 \times 10^4 P$, but some data are shown for $t_m = 12 \times 10^4 P$ (\blacktriangle). Solid circles (\bullet) show some of the quasistatic heating curves from Fig. 3. In panels (c) and (d) the growth time τ and the lag time τ_o are plotted in semi-log scale. Both times increase strongly as $\Gamma_q = 4.8$ is approached. The continuous line in panel (c) shows a linear fit, $\log(\tau/P) = a^* \Gamma_q + \tilde{a}$, with $a^* = 4.1 \pm 0.5$. The dashed line in panel (d) indicates the boundary below which clusters grow immediately after a quench.

In Fig. 4 we also present our data fitted by a stretched exponential growth law,

$$N_c(t) = N_\infty + (N_o - N_\infty) \exp\{-[(t - \tau_o)/\tau]^\alpha\}, \quad (1)$$

where N_∞ is the asymptotic number of particles in the solid phase and τ the growth time. N_o is the background “noise” in the measurement of the number of solid particles; in the liquid state, there are many small short-lived clusters that are considered as being composed of particles in a solid phase (see Fig. 2). Together with the exponent α and time lag τ_o , the quantities N_∞ , τ , and N_o are used as fit parameters. This stretched exponential law has been used in first-order phase transitions to model the growth of the stable phase into the metastable one [20]. It has also been used to describe the compaction of a sand pile under tapping [4]. In our case, the adjustment shown by the continuous lines in Fig. 4 is

very good. The exponent α fluctuates around $1/2$ as a function of Γ_q , as shown in Fig. 5(a) (data on the x axis correspond to realizations for which the phase separation was not achieved in the experimental observation time). In fact, the results that are discussed in what follows do not depend strongly on the fact that α can be left as a free parameter or fixed to $\alpha = 0.5$.

The dependence of N_∞ on Γ_q is shown in Fig. 5(b). The asymptotic fraction of particles in the solid phase, N_∞/N_c , decreases for high quenching accelerations, from ≈ 0.9 for $\Gamma_q = 3-3.4$ to ≈ 0.6 at $\Gamma_q \approx 4$. We notice that except for some experiments where we do not wait enough to overcome the time lag τ_o (data on the x axis), the value of $N_\infty(\Gamma_q)$ collapses with the one obtained for $N_c(\Gamma)$ by quasistatic heating, showing that we really perform an adiabatic modification of the forcing for the heating case with our quasistatic procedure.

In Figs. 5(c) and 5(d) we present τ and τ_o as functions of Γ_q . Our results show that both times increase strongly in a small range of Γ_q : about 2 orders of magnitude for Γ_q between 3.1 and 4.1. The longest measured growth and lag times, for $\Gamma_q \approx 4.1$, are $\tau \approx 3.5 \times 10^4 P = 350$ s and $\tau_o \approx 5 \times 10^4 P = 500$ s. If Γ_q is approached to $\Gamma_l = 4.8$, the lag time τ_o becomes larger than the measurement time t_m and no transition from the homogeneous fluid state to the coexistence between solid and fluid phases is observed. In the short parameter range where Eq. (1) can be verified, we obtain $\tau \sim \exp(a^* \Gamma_q)$, with $a^* = 4.1 \pm 0.5$. Concerning the time lag τ_o , we observe that it is highly variable; many more experiments seem necessary in order to obtain significant statistics. For $\Gamma_q < \Gamma_s = 3.4$, this time lag tends to a constant, $\tau_o \sim 1$ s. As we acquire images at 0.5 fps, this saturation seems artificial. In fact, after doing many realizations we conclude that for $\Gamma_q < \Gamma_s = 3.4$ the solid cluster seems to grow immediately with no delay. Notice that, defined this way, Γ_s is different and lower than Γ_c . Thus, our current measurements do not allow us to measure small values of τ_o with enough precision. However, for $\Gamma_q > \Gamma_s = 3.4$, τ_o is a few tenths of a second, and, despite the poorer statistics, a strong growth is observed. Finally, the strong increases for both τ and τ_o are the reason we cannot get closer to Γ_l within the experimental observation times. For example, for $\Gamma_g = 4.5$ and $\Gamma_q = 4.8$, the extrapolation for τ gives $\tau \sim 10^5 P \sim 1000$ s and $\tau \sim 4 \times 10^5 P \sim 4000$ s, respectively. Because τ_o also would increase significantly, then very long measurement times would be needed and particles would decrease significantly their magnetic interaction strength during these experiments.

IV. DISCUSSION AND CONCLUSIONS

In summary, quasistatic cooling and heating of a layer of dipolar interacting spheres is performed by slow changes of the driving acceleration. The system exhibits a hysteretic phase transition between a disordered liquidlike phase and an ordered phase. The ordered phase is formed by dense clusters, structured in an hexagonal lattice, coexisting with disordered grains in a liquidlike phase. By quenching the system in the vicinity of the transition, we study the dynamical growth of the ordered clusters, which can arise after a time delay. The time evolution of the number of particles in the solid-crystal phase is well fitted by a stretched exponential law.

The first point to discuss is why we do not observe particles in a state of branched chain, as reported in numerical simulations [14–16]. Indeed our filling fraction, $\phi = 0.59$, and the reduced temperature, $T^* \sim 0.4$, are not so far from the values used in Refs. [14–16]. However, we do not observe the branched state reported in these studies, at least not as a stable, stationary configuration. For our experiment, as mentioned in Sec. II, if a quench is done deeply into the solid phase, $\Gamma_q \sim 1$ –3, then many small solid clusters are formed quickly and many linear chains are present. However, this state eventually evolves to a more densely packed state, with almost no linear chains, in coexistence with the liquid phase. More systematic experiments should be performed to study properly this aging process. We conjecture that a stronger magnetic interaction might lead to favor stable linear chains.

Compared to numerical simulations, one of the major differences is in the vertical vibration imposed in our experiment to sustain particle motion. Indeed, instead of the 2D thermal motion used in numerical studies, a particle in the solid phase collides with the bottom and top plates during an excitation period. The vertical motion might disadvantage the formation of long chains, and compact clusters might be more stable under such driving. In addition, the fact that our experiments are done at higher density and with particles that undergo dissipative collisions probably helps to form denser 2D clusters as opposed to linear chains. Moreover, in contrast to numerical simulations, the magnetic dipole moments are probably not uniformly distributed in all the particles. Although it is really difficult to estimate the width of the dipole moments' distribution in our experiment, a fraction of them could be small enough to prevent binding.

The second point deserving discussion is the existence of the quasistatic hysteresis loop when the driving amplitude is slowly modified. A crucial point is that during a cooling ramp there is a specific driving, Γ_c , which depending on the particular magnetization history is between 3.5 and 3.9, below which solid clusters grow. Due to magnetization reduction and because τ and τ_o vary with driving amplitude, this specific boundary is very difficult to determine more precisely. How slow one should vary the driving depends on the time scales that are present in the system, that is, on τ and τ_o . The quench experiments show that, within the hysteresis loop, both times grow strongly with driving amplitude. These same quench experiments show the existence of another particular acceleration, Γ_s ($\lesssim \Gamma_c$), below which $\tau_o \approx 0$. This onset value seems to be better defined than Γ_c .

Our quasistatic increasing acceleration ramps show that the heating branch of the loop seems to be a stable, adiabatic branch. In particular, all quasistatic heating ramps follow the same curve and the critical driving above which solid clusters disappear, $\Gamma_l = 4.8 \pm 0.1$, is very reproducible. The fact that we are able to follow adiabatically this stable branch can be understood with the following reasoning.

- (1) A ramp starts at low Γ with a well-formed solid cluster (or clusters) in coexistence with the liquid phase.
- (2) The driving amplitude is increased by a small amount, which increases the system's kinetic energy (granular "temperature").
- (3) Particles in the solid phase but at the cluster's boundary will receive stronger collisions from those in the liquid phase, so the probability of getting ripped off increases.
- (4) This results in a cluster size reduction, more or less continuously as the driving is increased further.
- (5) Because the change from the one state to another occurs smoothly, the time it takes can be short.

The fact that $\Gamma_l > \Gamma_s$ demonstrates that there is a metastable region for which the system might stay in a completely fluidized state, but from which eventually a solid cluster will nucleate and grow until a stationary size is reached. Also, quench experiments done for $\Gamma_q = 3.4$ –3.9 show that the final cluster size is the same as that obtained for the heating ramp (N_∞/N collapses with N_c/N of the heating quasistatic loop). This shows that the cooling ramp branch of the quasistatic loop is not stable, implying that the cooling ramp was probably not done slowly enough. This is consistent with the fact that

for a given magnetic interaction strength, the value of Γ_c depends on the decreasing ramp rate. Because the number of solid particles has to grow from the background noise level to the final asymptotic one, waiting times much longer than τ_o are necessary. Another possible route for the metastable state characterization would be to study precursors through density and velocity correlations.

We now turn to the values of α used to fit experimental data with a stretched exponential law. At equilibrium, we would expect the exponent $\alpha = D + 1 = 3$ [20], where $D = 2$ is the spatial dimension, but instead we obtain $\alpha \approx 0.5$. Due to the anisotropy of the attractive force, of the special shape of the interface, and of the fact that most of the clusters start to grow from boundaries, one could assume that our experiment behaves more like a quasi-1D system, but even in this extreme case, we should obtain $D \geq 1$ and $\alpha \geq 2$. Moreover, one has to underline that we are in an out-of-equilibrium dissipative system. Other aspects can therefore play a role, like dissipation, which is probably different in the cluster and liquid phase, or the very particular thermalization imposed by vertical vibration. This effect could be especially important near the transition where a critical behavior can be expected. Actually, the exponent $\alpha < 1$ is measured in another out-of-equilibrium system: the slow compaction of granular packing by tapping [4], but the meaning of such a law is still under debate in this case. This issue deserves further study by changing the boundary shape (from square to circular), by doing the experiment in a viscous fluid to modify the dissipation, or by exciting the grains by vibration using colored noise with a broad frequency range.

Up to now we do not have a model to support the stretched exponential formula (1), which however appears to be a very convenient fit. At this stage of our understanding, fit parameters do not give much explanation about the phase separation physical mechanism. In order to build such a model one would have to consider the phase transition with a finite number of particles in a finite volume.

Finally, the combination of different dissipation and external driving on each phase leads us to conclude that these will not have the same efficiency in both phases. The output is

that the “granular” kinetic temperatures can be very different between the liquid and solid phases, as evident from our observations. This has an important effect on the intensity of fluctuations in each phase. For example, in the metastable region, the transition from the liquid state to the coexisting one can be achieved within the experimental time scales that are available. This transition occurs because the appropriate fluctuation occurs in the liquid state. However, the inverse transition has not been observed within the experimental observation times. We conjecture that once a particle is trapped in this solid state, it becomes very difficult to receive enough energy to escape. In the limit where one of the phases would be absolutely free of fluctuations, the system would fall into the absorbing phase transition category. This is one of the few out-of-equilibrium phase transitions that has been clearly identified experimentally, in particular, one realization belonging to the direct percolation universality class [2]. Therefore, it is tempting to propose our system as a candidate for the study of a quasiabsorbing phase transition. Indeed, our results share similarities with measurements performed between two liquid crystal turbulent phases [21], in which a hysteresis loop is observed between a turbulent phase stable at high excitation (called DSM2) and a quasiabsorbing state (called DSM1) observed at lower driving [22]. However, the relatively small size of our system, and our imperfect control on the spheres’ magnetization and therefore on the transition onset, makes very difficult any quantitative benchmark between our system with other studies exhibiting out-of-equilibrium quasiabsorbing phase transitions.

ACKNOWLEDGMENTS

We thank Cecile Wiertel-Gasquet, Vincent Padilla, and Corentin Coulais for valuable technical help and discussions. This research was supported by ECOS-CONICYT, Grant No. C07E07; Fondecyt, Grant No. 1120211; Anillo ACT 127; and Grant RTRA-CoMiGs2D. P.G. also acknowledge CONICYT for support.

-
- [1] S. Lübeck, *Int. J. Mod. Phys. B* **18**, 3977 (2004).
 - [2] K. A. Takeuchi, M. Kuroda, H. Chaté, and M. Sano, *Phys. Rev. Lett.* **99**, 234503 (2007).
 - [3] O. Pouliquen, M. Nicolas, and P. D. Weidman, *Phys. Rev. Lett.* **79**, 3640 (1997).
 - [4] G. Lumay and N. Vandewalle, *Phys. Rev. Lett.* **95**, 028002 (2005).
 - [5] S. Živković, Z. M. Jakšić, D. Arsenović, Lj. Budinski-Petković, and S. B. Vrhovac, *Granular Matter* **13**, 493 (2011).
 - [6] S. Aumaître, T. Schnautz, C. A. Kruelle, and I. Rehberg, *Phys. Rev. Lett.* **90**, 114302 (2003).
 - [7] A. Prevost, P. Melby, D. A. Egolf, and J. S. Urbach, *Phys. Rev. E* **70**, 050301(R) (2004).
 - [8] P. Melby *et al.*, *J. Phys.: Condens. Matter* **17**, S2689 (2005).
 - [9] M. G. Clerc, P. Cordero, J. Dunstan, K. Huff, N. Mujica, D. Risso, and G. Varas, *Nat. Phys.* **4**, 249 (2008).
 - [10] D. Lopez and F. Pétrélis, *Phys. Rev. Lett.* **104**, 158001 (2010).
 - [11] C. Laroche and F. Pétrélis, *Eur. Phys. J. B* **77**, 489 (2010).
 - [12] A. Kudrolli and D. L. Blair, *Phys. Rev. E* **67**, 021302 (2003).
 - [13] A. Kudrolli and D. L. Blair, in *The Physics of Granular Media*, 1st ed., edited by H. Hinrichsen and D. E. Wolf (Wiley-VCH, New York, 2005).
 - [14] T. Tlusty and S. A. Safran, *Science* **290**, 1328 (2000).
 - [15] P. D. Duncan and P. J. Camp, *Phys. Rev. Lett.* **97**, 107202 (2006).
 - [16] J. M. Tavares, J. J. Weis, and M. M. Telo, *Phys. Rev. E* **73**, 041507 (2006).
 - [17] N. Rivas, S. Ponce, B. Gallet, D. Risso, R. Soto, P. Cordero, and N. Mujica, *Phys. Rev. Lett.* **106**, 088001 (2011).
 - [18] G. Castillo, N. Mujica, and R. Soto, *Phys. Rev. Lett.* **109**, 095701 (2012).
 - [19] D. Blair and E. Dufresne, <http://physics.georgetown.edu/matlab/>
 - [20] M. Avrami, *J. Chem. Phys.* **7**, 1103 (1939); **8**, 212 (1940).
 - [21] S. Kai, W. Zimmermann, M. Andoh, and N. Chizumi, *Phys. Rev. Lett.* **64**, 1111 (2011).
 - [22] K. A. Takeuchi, *Phys. Rev. E* **77**, 030103(R) (2008).